Chapter 11

Longitudinal Vibration of Rods: Material Characterization and Experimental Dispersion Curves [1]

11.1. Introduction

Longitudinal rod vibrations seem an easy practical way to measure Young's modulus[2]. Dispersion curves (i.e. phase or group velocity versus frequency) are more difficult however to formulate on theoretical grounds. To take into account extensional displacement along rod axis, shear effect and transverse displacements, in order to formulate differential equations of motions by Hamilton variational principle, a displacement field must include three components of displacements. Higher order equations of motion are deduced (see [CHE 10], Chapter 7).

In this chapter, a number of experimental set-ups are presented. Isotropic metal material and composite material characterizations will be discussed. The principal theoretical results are succinctly presented in the appendices. Moreover, the problem of an experimental dispersion curves will be the main focus in this chapter.

Chapter written by Yves CHEVALIER and Jean Tuong VINH

1 This chapter uses large extracts from Touratier's dissertation for a mechanical engineer diploma at CNAM Paris.

2 In textbooks devoted to elementary dynamics of structures, the second order equation of motion is usually referred to.

Mechanical Characterization of Materials and Wave Dispersion: Instrumentation and Experiment Interpretation
Edited by Yvon Chevalier and Jean Tuong Vinh

11.2. Mechanical set-up

Figure 11.1 presents a suspension system using nylon strings. There are six attachment points on the rod and two strings at each point. This system is adopted to prevent parasitic transverse rod oscillations.

A preliminary vibration test is necessary to ensure that the contact lines between strings and rod do not influence the formation of nodes and antinodes on the rod. Modification of the contact lines must not influence resonance frequency. The sample must be long enough to obtain a large frequency range, particularly at lower frequencies (the rod length, L, should be of the order of 2–3 meters).

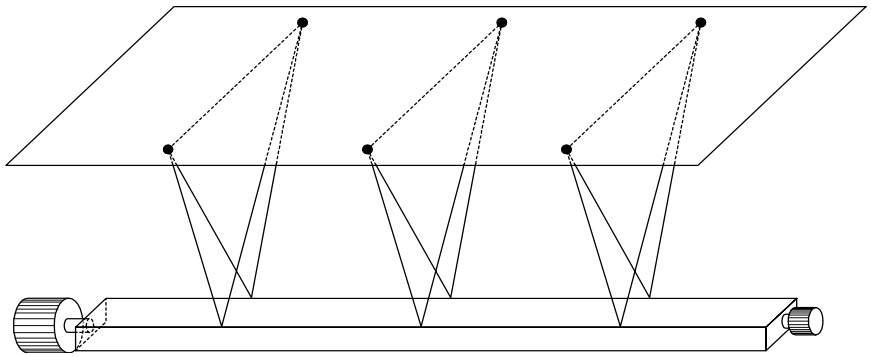

Figure 11.1. *Double strings at each attachment point on the ceiling prevent transverse parasitic transverse oscillations of the rod. The strings must be fine enough so that contact between them and the rod does not influence the formation of nodes and antinodes on the rod*

11.3. Electronic set-up

There are two classical measuring chains: one for the exciter and the other for the rod response.

11.3.1. *Magnetic exciter*

This type of transducer is used here because vibration of the rod does not necessitate a high level excitation power. A contactless magnetic exciter is maintained at a small distance from one of the rod's free ends[3]. The permanent magnetic force exerted on the rod is weak and has no influence on vibration of the rod itself. The frequency range reaches 100,000 Hertz.

3 We are interested in the dispersion curve in an elastic regime.

11.3.2. *Power amplifier*

The output impedance of the power amplifier should be of the order of 1000 Ω. The power amplifier has a large frequency range (from 0 to 200,000 Hertz).

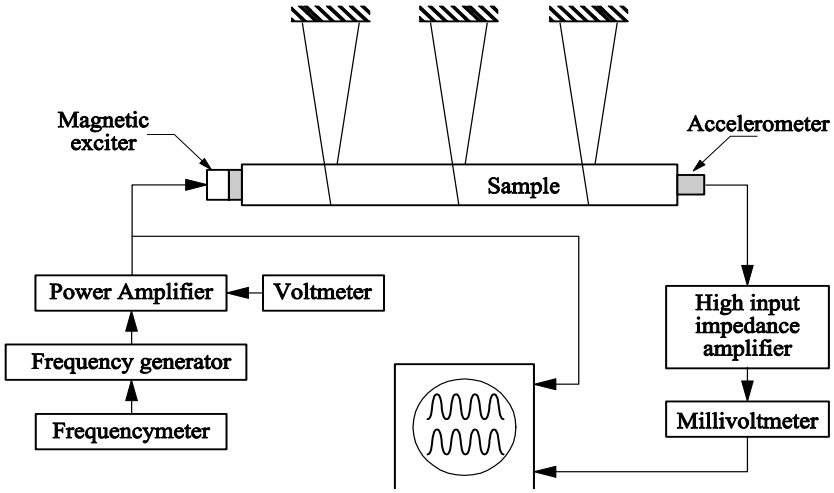

Figure 11.2. *Electronic set-up with two measuring chains: the oscilloscope serves only for visual observation. A digital chain of measurements including digital fast Fourier transforms (not presented in the figure) are used to obtain the transfer function between rod response (acceleration as the output signal on the right) and the input signal acceleration (on the left)*

11.3.3. *Frequency generators*

Two kinds of frequency generators are used successively. An analog frequency generator is used first to enable rapid sweeping and quick estimation of resonance frequency. The second generator, a digital and quartz piloted generator, is used to accurately adjust the resonance frequency of the sample.

11.3.4. *Accelerometer and preamplifier*

A lightweight, large frequency range accelerometer is used. The weight is of the order of several grams and it is glued directly to one end of the rod. The preamplifier has a high input impedance of $Zi \cong 10$ MΩ and a low output impedance of $Zo \cong 200$ Ω. This constitutes the usual characteristics of the accelerometer and its companion, the preamplifier.

11.3.5. *Oscilloscope*

An oscilloscope, with double sweeping and two inputs signals, allows the visualization of vibrations at various points on the rod.

11.4. Estimation of phase velocity

Measurements only furnish information concerning the resonance frequencies of the rod. As the rod is long and the rod mass is large compared to the mass of the accelerometer, the hypothesis of rod vibrations as an integer number p of a half wave is reasonable. Then, if the rod vibrates on its p^{th} eigenmode the corresponding wavelength Λ_p is:

$$\Lambda_p = 2L/p \qquad [11.1]$$

where p is an integer.

The wave number is:

$$k_p = 2\pi / \Lambda_p = \pi p / L \qquad [11.2]$$

The phase velocity is:

$$v = c = \Lambda_p N_p \qquad [11.3]$$

$$v = \frac{2L}{p} N_p \qquad [11.4]$$

With h as rod thickness, let us adopt a dimensionless wave number $\bar{k}$ and phase velocity $\bar{v}$:

$$\bar{k}_p = 1/(k_p h/2) \qquad = 1/(\text{kph} \qquad [11.5]$$

$$= = \bar{v} = \bar{c} = \frac{c}{c_3} = \frac{N_p}{pN_1} \qquad [11.6]$$

where c_3 is the longitudinal velocity at lower frequency N_1, and 3 is the rod axis direction, and N_p the eigenfrequency of order p.

11.4.1. *Experiments on metals: dispersion curves for isotropic materials*

Four long metallic rods were tested, where δ (the flatness factor) was defined as the ratio of width (b) to thickness (h), δ= b/h, β=1/δ=η1/. The four rods were:

– one steel rod ADX2[4] with square cross-section (δ=1)

Dimensions: 0.015×0.015× 3.722 m

218 resonance frequencies are estimated

– One steel rod ADX2 with rectangular cross-section (δ= 2)

Dimensions: 0.01× 0.02× 3.194 m

199 resonance frequencies are estimated

– One aluminum rod AU4G[5] with square cross-section (δ=1)

Dimensions: 0.01× 0.01×2.003 m

132 resonance frequencies are estimated

– Aluminum rod AU4G with rectangular cross-section (δ= 2)

Dimensions: 0.008×0.016×2.010 m

107 resonance frequencies are estimated

The frequency range obtained by manual sweeping is 30 < f < 158,000 Hz.

Figure 11.3 shows the dimensionless phase velocity $\overline{c_1} = c_L / c_E$ (where c_L is the longitudinal phase velocity, and $c_E = \sqrt{\frac{E}{\rho}}$) versus the dimensionless wave number $\overline{k_1}$, from equations [11.5] and [11.6].

4 ADX2 is the commercial name of the steel made in France.
5 Au4G is the commercial name of the aluminum made in France.

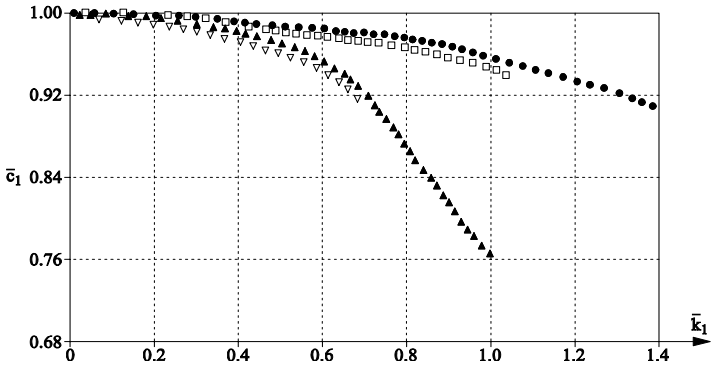

Figure 11.3. *Experimental dispersion curves of isotropic metallic materials for the first elastodynamic mode. Points are related to experimental values: $\delta = h/b$ represents the rod flatness defined as thickness on width, • Steel ADXE δ=1; ▲ Steel ADXE δ=2; □ Aluminum AU4G δ=1; and ∇ Aluminum AU4G δ= 2*

Not all the experimental values (there are 656) are presented in Figure 11.3. The dispersion depends essentially on the value β and phase velocity rapidly decreases with the increasing wave number $\overline{k_1}$. One of the practical conclusions is that, even for usual metallic materials, measurements over a large frequency range require caution when using elementary equations of motion which ignore dispersion phenomena.

11.4.2. *Experiments on composite materials: dispersion curves on transverse isotropic materials*

Anisotropic materials are made up of unidirectional long fibers with a polyester resin composite. Three kinds of composites were tested:

– composite rod (fiberglass E – polyester resin) with a circular cross-section of diameter $\phi = 15\text{x}10^{-3}$ m; length L=2.009m. Fiberglass percentage in volume: 72%;

– composite rod (fiberglass E – polyester resin) with square cross-section. Dimensions: 0.012× 0.012 × m3.006 m. Fiberglass percentage in volume: 65%;

– composite rod (fiberglass E – polyester resin) with rectangular cross-section. Dimensions: 0.008 × 0.02 × 3.003 m. Fiberglass percentage in volume: 65%.

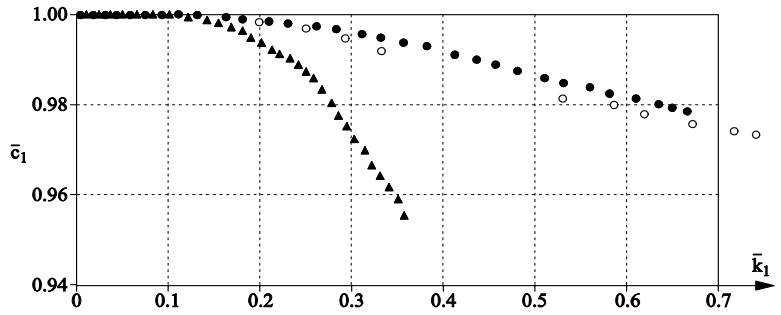

Figure 11.4. *Experimental dispersion curves for three transverse isotropic materials (first elastodynamic mode: fiberglass E – polyester resin, circular cross-section O; fiberglass E – polyester resin, square cross-section flatness δ b/h=1: •; and fiberglass E – polyester resin, rectangular cross-section: flatness δ= 2.5: ▲*

11.4.3. *Confrontation theory - experiment for metals*

To evaluate the validity of this approximate first order theory, it is interesting to compare with experimental results. For the metallic rods presented above, (section 11.4.1), Poisson's numbers for steel and aluminum are ν_{steel} = 0.28 and $\nu_{Aluminum}$ = 0.33 respectively.

Figure 11.5 shows that the theoretical curves are only closely approached by experimental curves for the sample with a square cross-section. By contrast, dispersion is predominant for the rectangular cross-section δ=2.

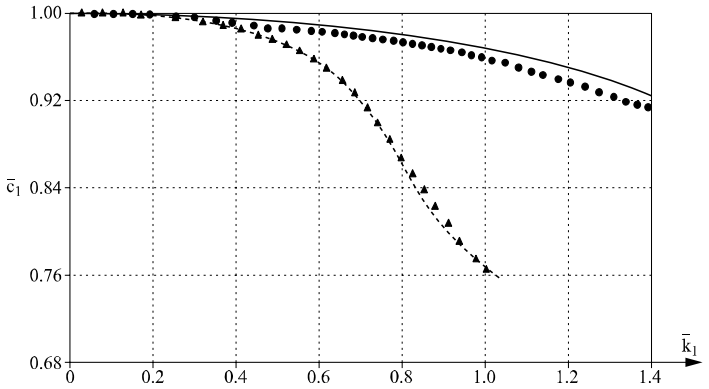

Figure 11.5. *Dispersion curves for isotropic materials: δ is the rod flatness defined as the ratio b (wdith) on h (thickness) steel ADXE (square section with δ=1) and rectangular section (δ=2): o; with experimental points δ=1, ▲, experimental points with δ= 2, --- continuous curves.* ν_{steel} *= 0.28,*$\nu_{alumi.}$ *= 0.33*

11.4.4. *Confrontation theory: an experiment for composite materials*

Figure 11.6 shows weak discrepancies between theoretical dispersion curves for fiberglass-epoxy resin composites. We consider that the higher order approximation theory presented elsewhere [CHE 10, Chapter 7] seems appropriate for application here, without recourse to more complicated or sophisticated theories.

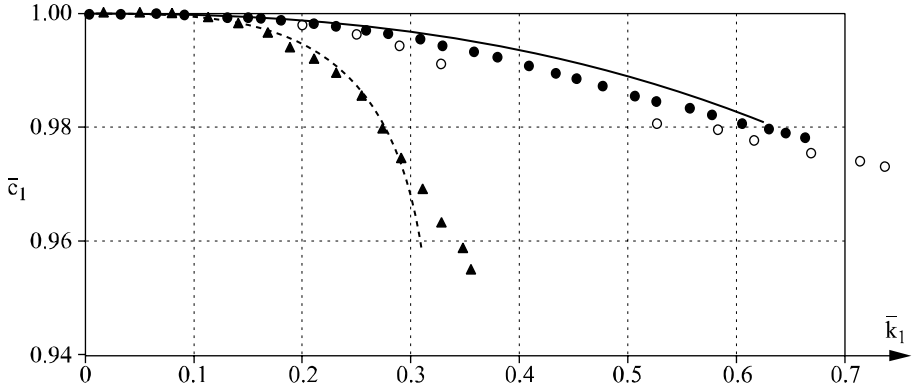

Figure 11.6. *Dispersion curves for composites– confrontation theory - experiment.*
▲ = Fiberglass polyester resin β=2/5, δ=5/2 (rectangular cross-section);
●=Fiberglass - polyester resin β=δ=1 square cross-section;
O = Fiberglass - polyester resin – circular cross-section;
--- *Continuous line curves- theory-equations [7.69a] and [7-69b] of chapter*[6]

Touratier's theory of longitudinal vibration of rod applicable to composite materials is presented in Appendixes 11A, B, C, D.

11.4.5. *Frequency spectrum for metals*

The frequency spectrum is often used in acoustics to represent the curve $\omega = \omega(k)$. From this curve, phase velocity $v_p = \omega/k$ and group velocity $v_g = d\omega/dk$ are easily and precisely obtained. In the frequency spectrum, dimensionless variables $\overline{\omega}_1$ and $\overline{k_1}$ can be used. If the dimensionless wave number $\overline{k_1}$ is complex[7], we can draw the curve $\overline{\omega_1} = \overline{\omega_1}(\text{Real } \overline{k_1})$.

---

6 In Chapter 15, a more elaborate theory using the Hellinger-Reissner variational principle is used. It is applicable to higher frequency ranges and higher elastodynamic modes.

7. This does not necessarily mean that we have to deal with viscoelastic materials. We can, in this case, have wave attenuation even in elastic media.

In Figure 11.7, a real branch of the frequency spectrum is represented. Even for an isotropic material, dispersion is pronounced. Its departure from elementary theory begins with $\overline{k_1} \cong 0.6$.

11.4.6. *Frequency spectrum of some composites materials:* $\overline{\omega_1} = \overline{\omega_1}\ (Real\ \overline{k_1})$

For the first elastodynamic mode, discrepancies between elementary theory and experiments begin with Real ($\overline{k_1}$) = 0.4. A confrontation theory experiment for a composite material shows that the extension of Volterra's theory to composite materials by Touratier is a success, at least for low values of relative wave number. In Figure 11.8, the dispersion phenomenon is examind with frequency spectra – with$\omega k = \omega k(k)$ representing the variation of dimensionless circular frequency versus the dimensionless wave number is drawn for four different composite materials.

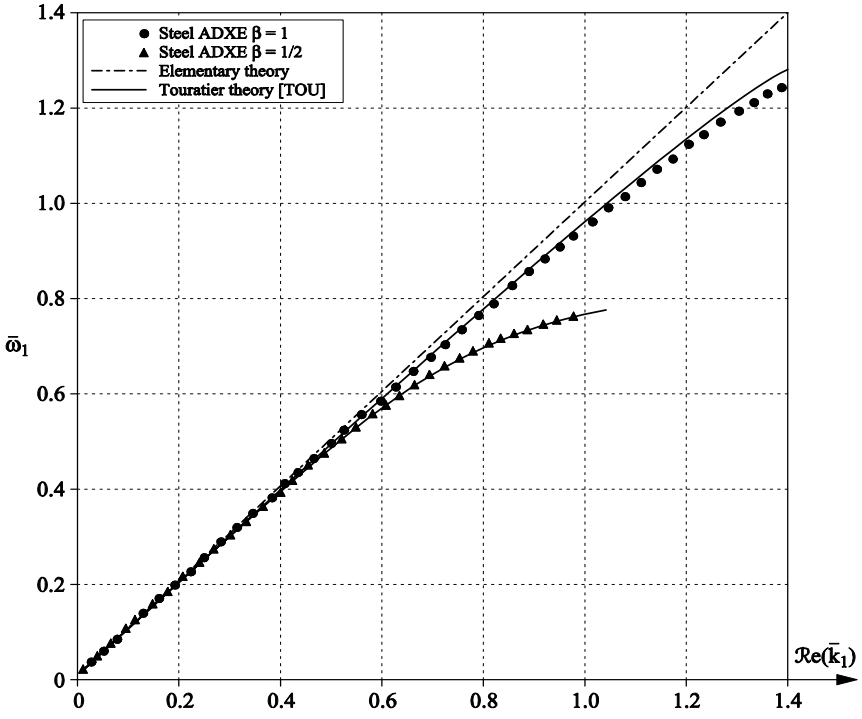

Figure 11.7. *Real branch of frequency spectrum associated to first elastodynamic mode*

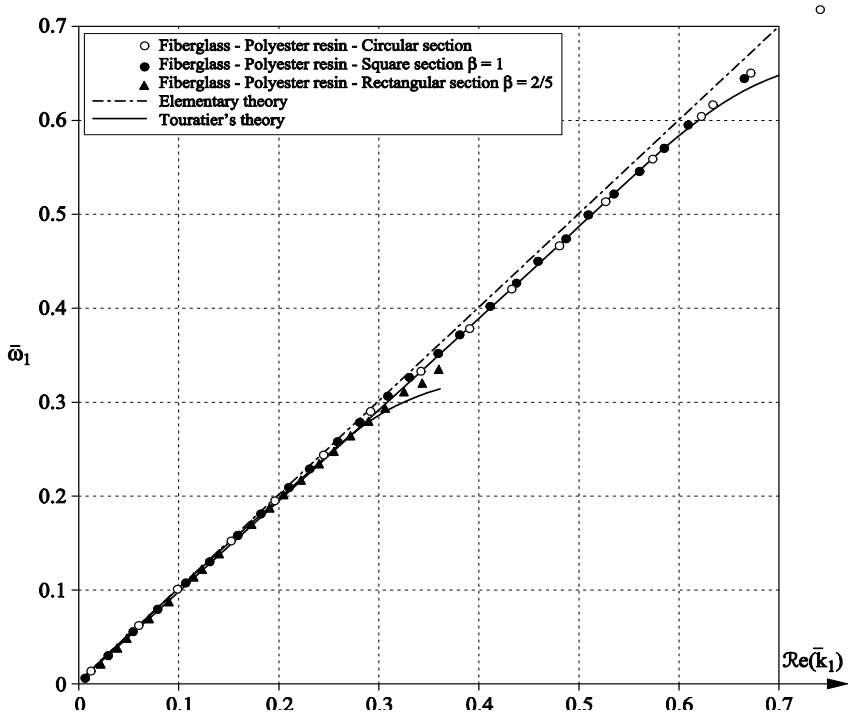

Figure 11.8. *Confrontation theory-experiment with composite materialfibrefiberglass-polyester resin*

11.5. Short samples and eigenvalue calculations for various materials

For long rods, the ends being free, it is possible to assimilate the rod as an integer number of half length and the calculation of frequency spectra is easy. For a short sample, the boundary conditions at both ends become predominant with respect to the rod mass itself. Short samples are usually adopted for material characterization. However, precautions must be taken not only for the sample length but also for the influence of sample slenderness on the eigenvalues.

When exploring rod vibration frequencies of short samples in a large frequency range, discrepancies between results obtained by elementary and more elaborate theories (for example, Touratier's theory) may be large. Errors with respect to experimental results are presented in the next section.

11.5.1. *Flow charts to evaluate reduced eigenvalues*[8]

Elementary equations of motion and higher order equations using a simple displacement field as well as eigenvalues depending on the boundary conditions can be found elsewhere. Flow charts are discussed here, and Figure 11.9 shows the flow chart to evaluate eigenvalues in the framework of elementary theory. Figure 11.10 concerns Touratier's theory.

11.5.2. *Discrepancies between elementary theory and Touratier's theory*

The discrepancy is defined as:

$$\bar{e_t} = \frac{|\omega - \omega'|}{\omega}, \qquad [11.7]$$

where ω is the circular eigenfrequency obtained by Touratier's theory, and ω' the circular eigenfrequency obtained by elementary theory.

Figure 11.12 shows the discrepancies defined by [11.7] versus p, the integer number indicating the eigenvalue rank. With increasing value of p, the discrepancy increases. For a fiberglass–epoxy resin composite, the discrepancy is more pronounced, which shows the limit of elementary theory for applications.

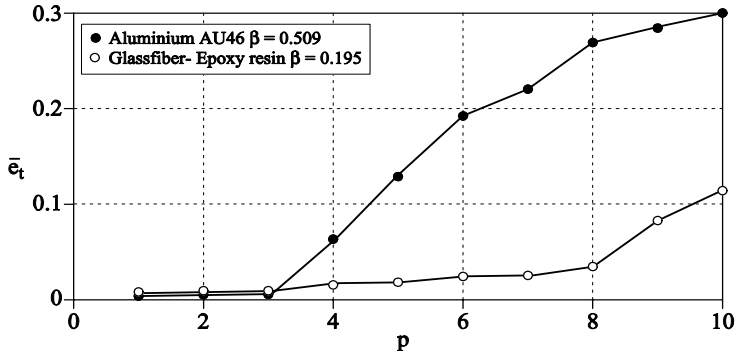

Figure 11.19. *Comparison between elementary theory and Touratier's theory. Discrepancy versus the eigenvalue rank p- $\bar{e_t}$ is given in [11.7]. Aluminum AU4G β=0.509, δ=1/β=1.96 – ●-●-●-; fiberglass-epoxy resin β =0.195, δ =1/β= 5.13– **o -- o***

8 Details on the theory can be found in Chapter 6 [CHE 10].

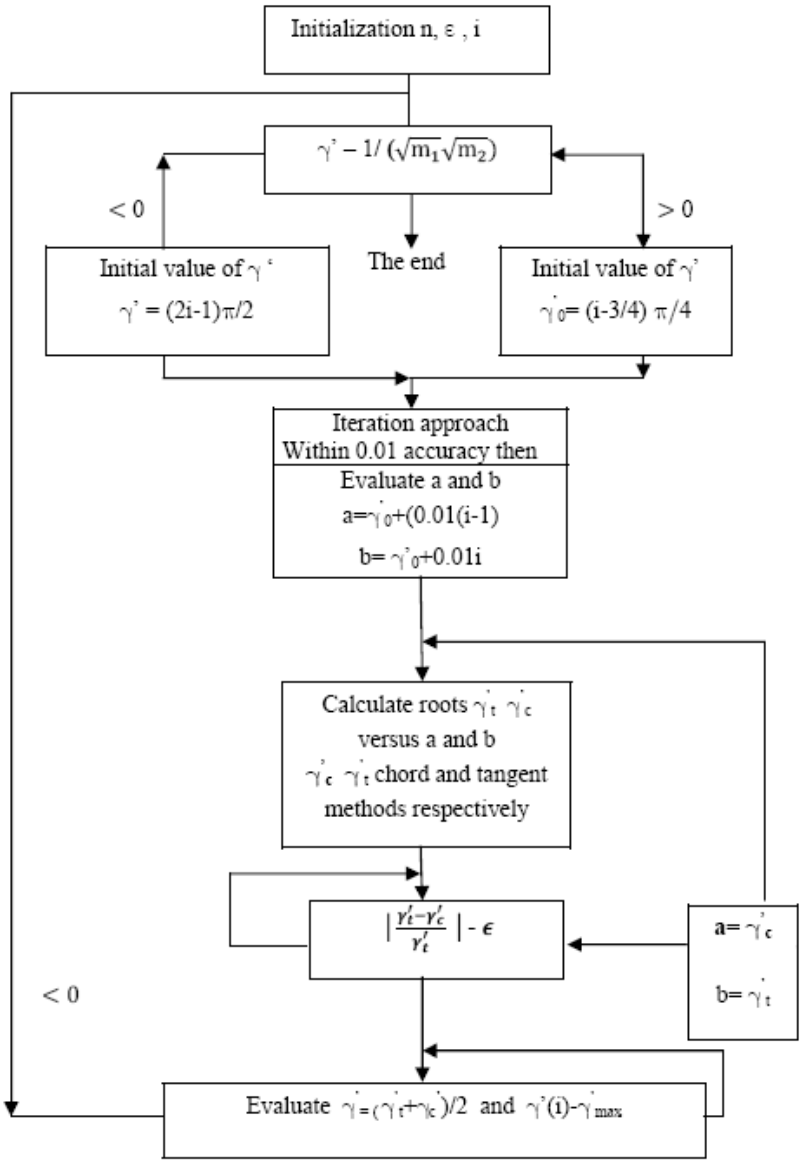

Figure 11.10. *Flow chart of eigenvalue calculation by elementary theory*

11.6. Experimental results interpreted by the two theories

The following parameters are used in the data presented in tables.

$$\overline{e_C} = \frac{N_C - N_M}{N_M} \quad [11.8]$$

$$\overline{e_E} = \frac{N_E - N_M}{N_M} \quad [11.9]$$

where N_E is the eigenfrequency by elementary theory, N_M the measured eigenfrequency, and N_C is Touratier's eigenfrequency.

In the tables presented below, the following notation is used:

$$\alpha_1^2 = \frac{C_{11}}{C_{44}}; \quad \alpha_2^2 = \frac{C_{12}}{C_{44}}; \quad \alpha_3^2 = \frac{C_{33}}{C_{44}}; \quad \alpha_4^2 = \frac{C_{13}}{C_{44}}$$

= ;;= ;; = ; = where α'^2 is the coefficient of the second derivative presented in following equation and is defined as follows:

$$\alpha'^2 = \frac{1}{X_{44}^2}\left[X_{33}^2 - \frac{4}{3}\frac{X_{13}^2}{(X_{11}^2 + X_{12}^2)}\right] = \alpha_3' - \frac{4}{3}\frac{\alpha_4^4}{(\alpha_1^2 + \alpha_2^2)} \quad [11.10]$$

$$X_{ij}^2 = C_{ij}/\rho \quad [11.11]$$

2a=h (thickness)

$$\delta = \frac{b(width)}{h(=2a)} = \frac{1}{\beta} \text{ flatness factor;} \quad \delta_L = \frac{L(length)}{h(thickness)} \text{ slenderness factor} \quad [11.12]$$

11.6.1. *Steel ADXE*

Elastic characteristics:

$$\alpha_1^2 = 3.273; \quad \alpha_2^2 = 3.273; \quad \alpha_3^2 = 1.273; \quad \alpha_4^2 = 1.273; \quad \alpha'^2 = 2.7977$$

Geometrical characteristics:

$\beta = 0.495$; $\delta_L = 40.65$; $2a = 9.8 \times 10^{-3}$ m

p (mode rank)	N_M (Hz)	N_C(Hz)	N_E(Hz)	$\overline{e_C}$	$\overline{e_E}$
1	12888	12920	12931	0.002	0.003
2	25742	25834	25861	0.004	0.005
3	38371	38579	38795	0.005	0.011
4	50204	51212	51725	0.020	0.030
5	63294	63841	64656	0.009	0.021
6	77146	76334	77590	0.010	0.006
7	88517	87480	90524	0.012	0.023
8	99069	98429	103455	0.027	0.044
9	107935	109283	116389	0.012	0.078
10	114735	115711	129327	0.008	0.127
11	123848	122852	142262	0.008	0.149
12	133148	132850	155196	0.002	0.165

Table 11.1. *Eigenfrequencies (measured) N_M , (calculated) N_C after Touratier's theory applied to short steel rod. $\overline{e_C}$,$\overline{e_E}$ are discrepancies defined in [11.8] and [11.9], p designates the rank of eigenmode; β and δ_L are given by [11.12], 2a =h (thickness). α_1, α_2, α_3, α_4, α' are reproduced above*

11.6.2. *Aluminum AU4G*

Elastic characteristics:

$\alpha_1^2 = 3.941$; $\alpha_2^2 = 1.941$; $\alpha_3^2 = 3.941$; $\alpha_4^2 = 1.941$; $\alpha'^2 = 3.087$

Geometrical characteristics:

$\beta = 0.509$; $\delta_L = 49.80$; $2a = 8.1 \times 10^{-3}$ m

Reduced masses $\overline{m_1} = 0$; $\overline{m_2} = 0.0287$; mass density $\rho = 2.805 \times 10^3$ kg/m^3

p (mode rank)	N_M (Hz)	N_C (Hz)	N_E(Hz)	$\overline{e_C}$	$\overline{e_M}$
1	12383	12380	12459	0.0002	0.006
2	24725	24690	24922	0.001	0.008
3	36487	36949	37393	0.013	0.025
4	47081	49020	49885	0.041	0.059
5	56507	61213	62388	0.083	0.104
6	67451	72539	74912	0.075	0.111
7	78015	85280	87461	0.093	0.121
8	89193	96605	100026	0.083	0.121
9	100296	104122	112611	0;038	0.123
10	110544	113060	125212	0.023	0.133
11	120037	119936	137765	0.001	0.148
12	127056	127499	150416	0.003	0.184
13	132091	132999	163078	0.007	0.234
14	140217	139875	175753	0.002	0.253
15	144361	143313	188441	0.007	0.305

Table 11.2. *Measured eigenfrequencies N_M , calculated frequencies N_C (Touratier's theory), N_E (elementary theory) for short rod with rectangular cross-section – Material: aluminum – discrepancies between measured and theoretical frequencies, equations [11.8] and [11.9]– subscript E: elementary theory; β, δ_L are given by [11.12] 2a=h (thickness)- α_1' , α_2' ,α_3', α_4^2, α^2 are given by [11.10] and repeated above*

11.6.3. *Fiberglass–polyester resin*

Elastic characteristics:

$\alpha_1^2 = 2.9454$, $\alpha_2^2 = 0.6502$, $\alpha_3^2 = 7.2628$, $\alpha_4^2 = 0.8566$; $\alpha'^2 = 6.9907$

Geometrical characteristics:

$\beta = 0.991$; $\delta_L = 38.21$; 2a=h=11.6.103kg/m^3

Mass characteristics $\overline{m_i}$ = mi/M, M rod mass:

$\overline{m_1}$ =9.9.10-4 , $\overline{m_2}$ = 0.0384 , mass density $\rho = 2.008 \times 10^3$ kg/ m^3

p (mode rank)	N_M (Hz)	N_C (Hz)	N_E(Hz)	$\overline{e_C}$	$\overline{e_E}$
1	9632	9789	9788	0.016	0.019
2	19328	19536	19536	0.011	0.016
3	28733	29364	29487	0.022	0.026
4	37754	39152	39357	0.037	0.042
5	45997	47030	49253	0.022	0.071
6	54298	58560	59175	0.078	0.090
7	64023	68186	69127	0.065	0.080
8	71918	72238	79104	0.004	0.100
9	80731	78824	89065	0.024	0.103
10	89470	86930	99097	0.028	0.108
11	97908	93515	109146	0.045	0.115
12	105646	98075	119211	0;072	0.128
13	112273	103140	129286	0.081	0.151

Table11.3. *Measured eigenfrequencies N_M, calculated eigenfrequencies N_C (Touratier's theory), calculated eigenfrequencies N_E (elementary theory) – discrepancies between measured and theoretical frequencies defined in [11.8] ang [11.9]- p is the eigenmode rank. β ,δ_L are given by [11.12] , 2a=h=(thickness) α_1, α_2 , α_3 , α_4 , α'^2 are given by [11.10]*

11.6.4. *Fiberglass–polyester resin*

Elastic characteristics:

α_1^2 =2.9454; α_2^2 =0.6502; α_3^2 = 7.2628; α_4^2 = 0.8566 ; α'^2 = 6.9907

Geometrical characteristics:

β = 0.43; δ_L = 56.62 : 2a=h= 7.7 x 10^{-3} m

Reduced masses $\overline{m_i}$ = mi / M, M rod mass:

$\overline{m_1}$ = 0.0011 ,$\overline{m_2}$= 0.0364; mass density ρ= 1.945 x 10^3 kg/ m^3

p (mode rank)	N_M (Hz)	N_C (Hz)	N_E (Hz)	$\overline{e_C}$	$\overline{e_E}$
1	9 903	9963	9997	0.006	0.009
2	19805	19971	20000	0.008	0.010
3	29057	29953	30023	0.031	0.033
4	36940	39791	40066	0.077	0.085
5	44534	49261	50132	0.106	0.126
6	53038	55152	60228	0.040	0135
7	61079	61042	70347	0.001	0.152

Table 11.4. *Measured eigenfrequenciesN_M, calculated eigenfrequencies by Touratier's theory N_C, calculated eigenfrequencies (elementary theory) N_E, discrepancies between measured and theoretical frequencies defined in [11.8] and [11.9], p is the rank of eigenmode. β,δ_L are given by [11.12], 2a=h (thickness);α_1', α_2' ,α_3', α_4', a^2 are reproduced above*

11.6.5. *Fiberglass–epoxy resin*

Elastic characteristics:

α_1^2 =3.1076; α_2^2=1.3715; α_3^2 = 7.8802; α_4^2 = 0.9722; α'^2= 7.5988

Geometrical characteristics:

β= 0.95; δ_L = 98.47 ; 2α = h thickness = 3.8 x 10^{-3} m

Reduced masses: $\overline{m_i}$ = mi / M, M rod mass :

$\overline{m_1}$ = 0.0011; $\overline{m_2}$ = 0.4404; ρ mass density = 1.869 x 10^3 kg/m^3

p (mode rank)	N_M (Hz)	N_C (Hz)	N_E (Hz)	$\overline{e_C}$	$\overline{e_E}$
1	9140	9274	9539	0.015	0.044
2	19701	20835	20896	0.057	0.061
3	31154	30228	33097	0.030	0.062
4	42600	45402	45605	0.066	0.070
5	54256	58047	58226	0.070	0.073
6	65918	70692	70913	0.072	0.076
7	77130	83489	83632	0.082	0.084

Table 11.5. *Measured eigenfrequencies N_M, calculated eigenfrequencies N_C, Touratier's theory, calculated eigenfrequencies N_E (elementary theory) – discrepancies between measured and calculated frequencies see [11.8] and [11.9]; β ,δ_L are given by [11.12] and reproduced above*

11.6.6. *Fiberglass–epoxy resin*

Elastic characteristics:

$\alpha_1^2 = 0.372$, $\alpha_2^2 = 1.3715$, $\alpha_3^2 = 7.8802$, $\alpha_4^2 = 0.9722$, $\alpha^{\prime 2} = 7.5988$

Geometrical characteristics:

$\beta = 0.372$, $\delta_L = 98.42$, 2a=h (thickness) = 3.8×10^{-3}m

Reduced masses ($\overline{m_i}$ =mi/M), M: rod mass:

$\overline{m_1}$ = 8.1.10-4 , $\overline{m_2} = 0.1718$, rod mass density $\rho = 1.869 \times 10^3$ kg/m^3

p (mode rank)	N_M (Hz)	N_C (Hz)	N_E (Hz)	$\overline{e_C}$	$\overline{e}_E$
1	10610	10982	11033	0.035	0.040
2	21490	22447	22523	0.044	0.048
3	32442	34409	34462	0,061	0.062
4	43656	44898	46739	0.028	0.071
5	54941	58952	59192	0.073	0.077
6	66747	71052	71730	0.064	0.075
7	78067	83153	84367	0.065	0.081
8	89176	91404	97036	0.025	0.088
9	100784	100204	109737	0.006	0.089
10	109767	107355	122443	0.022	0.115

Table 11.6. *Measured eigenfrequencies N_M, calculated eigenfrequencies N_C (Touratier's theory), calculated eigenfrequencies (elementary theory) – discrepancies between measured and calculated frequencies see [11.8] and [11.9]; β ,δ_L are given by [11.12], 2a=h (thickness), α', α', α', α_4,$a^2$are given by Touratier[TOU 78] and reproduced above*

11.6.7. *Fiberglass–epoxy resin*

Elastic characteristics:

$\alpha_1^2 = 3.1076$, $\alpha_2^2 = 1.3715$, $\alpha_3^2 = 7.8802$, $\alpha_4^2 = 0.9722$, $\alpha^{\prime 2} = 7.5988$

Geometrical characteristics:

$\beta = 0.195$, $\delta_L = 98.37$, 2a=h (thickness) = 3.8×10^{-3} m

Reduced additional mass ($\overline{m_i}$ = mi/M, M rod mass):

$\overline{m_1} = 0.0027$, $\overline{m_2} = 0.0905$, rod mass density $\rho = 1.869 \times 10^3$ kg/m^3

p (mode rank)	N_M (Hz)	N_C (Hz)	N_E (Hz)	$\overline{e_C}$	$\overline{e_E}$
1	11332	11717	11750	0.034	0.037
2	22334	23482	23617	0.051	0.057
3	32205	35491	35648	0.102	0.107
4	41487	44895	47846	0.082	0.153
5	51943	52945	60159	0.019	0.158
6	59641	60644	72606	0.017	0.217
7	67466	69744	85123	0.034	0262
8	77701	76744	97692	0.012	0.257
9	90275	85493	110280	0.053	0.222
10	101118	94593	122938	0.064	0.216

Table 11.7. *Measured eigenfrequencies N_M, calculated eigenfrequencies N_C (Touratier's theory), calculated eigenfrequencies N_E (elementary theory) – Discrepancies $\overline{e_C}$, $\overline{e_E}$ defined in [11.8] and [11.9]. β, δ_L are given by [11.12], 2a =h (thickness), α_1, α_2, α_3, α_4 , α^2 are given by Touratier [TOU 78] and reproduced above*

11.6.8. *Carbon fiber–epoxy resin (two rods with different characteristics)*

11.6.8.1. *Case (a): carbon fiber-epoxy resin*

Elastic characteristics:

$\alpha_1^2 = 1.8226$, $\alpha_2^2 = 0.9652$, $\alpha_3^2 = 4.2017$, $\alpha_4^2 = 0.7530$, $\alpha^{\prime 2} = 3.9305$

Geometrical characteristics:

$\beta = 0.215$, $\delta_L = 211.04$, 2a=h (thickness) = 2.3×10^{-3} m

Reduced additional mass $\overline{m_1} = 0.0012$, $\overline{m_2} = 0.2618$

Rod mass density $\rho = 1.484 \times 10^3 kg/m^3$

P (mode rank)	N_M (Hz)	N_C (Hz)	N_E (Hz)	$\overline{e_C}$	$\overline{e_E}$
1	15600	15518	15652	0.005	0.003
2	29335	28409	32703	0.031	0.115
3	44257	43688	50798	0.013	0.148

Table 11.8(a) *The table concerns the same composite material. Geometrical characteristics and reduced masses are different for the two rods. Measured eigenfrequencies N_M; calculated eigenfrequencies N_C; after Touratier's theory, N_E; calculated eigenfrequencies N_E after elementary theory. β, δ_L are given by [11.12], 2a=h (thickness). α_1, α_2, α_3, α_4, α^2 are given by [TOU 79], reproduced above*

11.6.8.2. *Case (b): carbon fiber-epoxy resin*

Elastic characteristics:

$\alpha_1^2 = 1.8226$, $\alpha_2^2 = 0.9652$, $\alpha_3^2 = 4.2017$, $\alpha_4^2 = 0.730$, $\alpha^{\prime 2} = 3.9305$

Geometrical characteristics:

$\beta = 0.120$, $\delta_L = 211.04$, 2a=h(thickness)= 2.3×10^{-3} m

Reduced additional mass $\overline{m_1} = 0.0045$, $\overline{m_2} = 0.2618$

Rod mass density $\rho = 1.484 \times 10^3$ kg/m^3

p (mode rank)	N_M (Hz)	N_C (Hz)	N_E (Hz)	$\overline{e_C}$	$\overline{e_E}$
1	15194	15209	16830	0.001	0.108
2	28134	28623	34170	0.017	0.214
3	43537	43426	52093	0.002	0.196
4	60877	61004	70427	0.002	0.157
5	70200	70506	89044	0.004	0.268

Table 11.8(b). *See caption for Table 11.8(a)*

An examination of all the tables presented above shows that:

– for metals, the relative discrepancies between elementary theory and experiment are of the order of 0.1 up to the fifth eigenmode. Beyond that limit, the

discrepancies increase rapidly with the eigenmode rank. Touratier's theory gives a reasonable discrepancy of less than 0.01;

– for composite materials, the discrepancy strongly depends on the ratio of the Young's modulus E_z to the shear modulus G_{xz}, (z being the rod axis). This ratio can reach or exceed 40. Strong dispersion of the elastic wave gives rise to large errors if elementary theory is used. Touratier's theory gives good results with weak discrepancies. However, the adequation theory-experiment necessitates a more elaborate theoretical framework.

11.7. Influence of slenderness ($\delta_L = 2L/h$) on eigenfrequency

Figure 11.11 shows the influence of slenderness on the reduced eigenfrequency defined as:

$$\overline{\omega} = \frac{a\omega}{c_3}$$

where ω is the circular eigenfrequency, a=h/2 half thickness, c_3 phase velocity in direction 3 of the rod axis. The material tested was steel. The rod has transverse dimensions: $0.01 \times 0.02\ m.2$ with $\beta = 1/\delta = 1/2$. The first ten eigenmodes are retained. With slenderness $\delta_L < 100$, large discrepancies are observed.

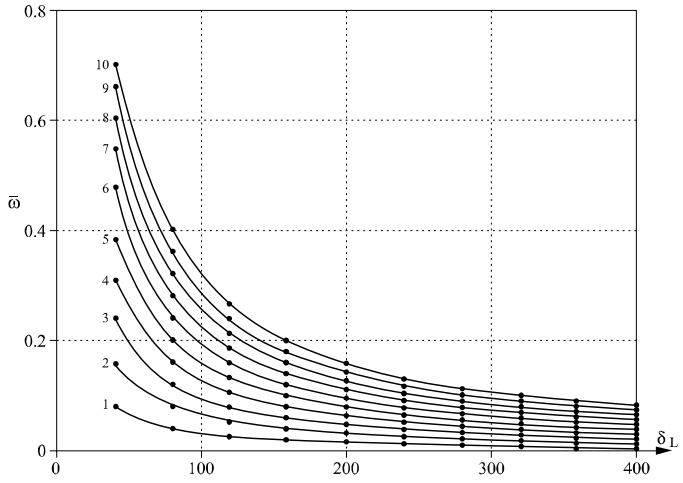

Figure 11.11. *Reduced circular eigenfrequency versus slenderness δ_L =2L/h (L rod length, h thickness) Material: steel. The ten curves concern the first ten eigenmodes whose rank is indicated on each curve. Dots ● are experimental points, whilst continuous lines are obtained from Touratier's theory*

11.8. Experimental results obtained with short rod

Figure 11.12 concerns two materials: steel and a carbon fiber composite. Even with a short rod the mean discrepancy $\overline{e_C}$ obtained with Touratier's theory is of the order of 3% for metal.

With the composite material, the error is large under elementary theory. For such a type of material, elementary theory is not acceptable.

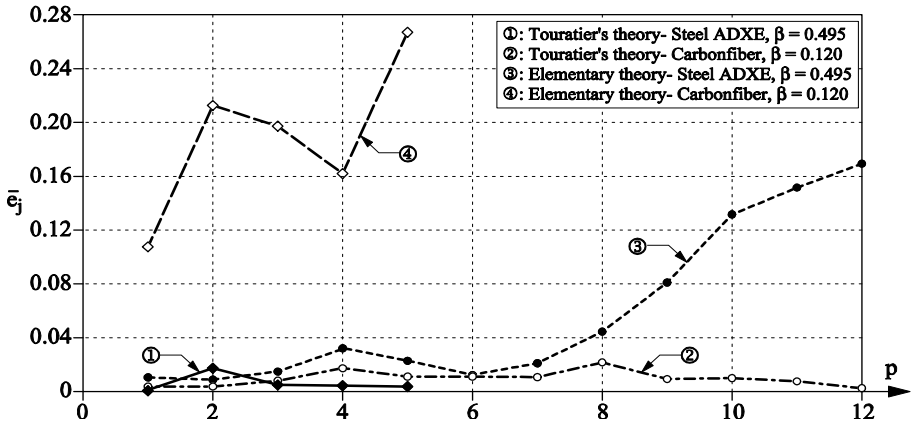

Figure 11.12. *Relative errors on eigenfrequencies versus eigenmode rank: 1. Touratier's theory – steel ADXE [TOU 79], $\beta=1/\delta=0.495$; 2. Touratier's theory – carbon fiber composite $\beta=1/\delta=0.120$; 3. elementary theory – steel ADXE, $\beta=1/\delta=0.495$; 4. elementary theory – carbon fiber composite, $\beta=1/\delta=0.120$.*

11.9. Concluding remarks

The following remarks can be drawn from elaborating Touratier's theory of extensional waves in rods.

11.9.1. *Material characterization*

11.9.1.1. *Elementary theory*

Elementary theory is largely used in industry and in engineering science to describe the elastic behavior of rods. However, the limitation of this theory must be known in material characterization. If we follow the trend in the fabrication of apparatuses in industry, isothermal tests are increasingly being adopted to the detriment of the test at different temperatures. Inevitably, a large frequency range is thus adopted. The problem is to know whether the important problem of wave

dispersion is taken into account. Adoption of elementary theory gives rise to large errors at higher frequency particularly when using longitudinal rods.

11.9.1.2. *Higher approximation theories*

When characterization is expected in a large frequency range, ignorance of the longitudinal wave dispersion might give rise to large errors in the calculation of the elastic modulus. In this chapter, a variety of materials are tested and many important parameters have been presented and discussed. They include:

– the ratio of the Young's modulus to the shear modulus; wave dispersion is strongly dependent on this ratio;

– slenderness: length / half thickness (2L/h); when slenderness is small (as is the case for short rods), dispersion becomes important and recourse to higher approximation theory enables better results to be obtained;

– transverse geometrical parameter-cross-section flatness; for rectangular cross-sections, the square cross-section gives the less pronounced wave dispersion, everything else being equal.

11.9.1.3. *Elastic characterization of materials*

If only the elastic characterization of a material is desired, try to use the lowest frequency range in which the wave dispersion is not important and, if possible, choose a square cross-section instead of a rectangular cross-section (see above).

11.9.1.4. *Viscoelastic characterization of materials*

When using longitudinal rod vibration to evaluate complex Young's modulus, it is important to ascertain that the wave dispersion, in the adopted frequency range, can be neglected. If not, the experimenter has to deal with two phenomena: (a) geometrical (wave) dispersion and (b) viscoelastic dispersion.

These two phenomena might counter-balance each other or strengthen each other. The difficulty resides in the fact that recourse to higher approximation theory uses more than one viscoelastic moduli (Young's modulus and shear modulus). Some simplifying assumptions are then adopted. For example, for isotropic materials, Poisson's number is supposed to be constant:

$$E/G = 2(1+\nu)$$

This hypothesis has to be confirmed in the adopted frequency range.

11.9.2. *Experiments in applied elastodynamics to show the influence of wave dispersion on the dynamic behavior of elastic rods*

11.9.2.1. *Mechanical set-up*

In this chapter, we show that it is not difficult for students to realize a mechanical set-up. If a long steel rod is used, more than 100 eigenfrequencies can be evaluated and curves, such as in Figure 11.5, are obtained with various value of eigenvalues.

11.9.2.2. *Comparison theory: experiment*

As viscoelastic behavior of steel is neglected, elementary theory and Touratier's theory can be successively adopted for computation; see the continuous curves in Figures 11.5 and 11.6.

11.9.3. *Position of Touratier's theory in longitudinal rod vibration*

The main ideas of Touratier's theory are summarized below.

11.9.3.1. *Longitudinal wave dispersion in rods*[9]

This is the most difficult phenomenon to understand. Many groups of theories have been proposed. Schematically, we can distinguish a number of main groups:

(a) *Linear functions of coordinates for the displacement field* (Love-Rayleigh's lateral inertia correcting term). Bishop proposed an inertia correction and shear correction; unfortunately his equation is not able to describe the wave dispersion trend correctly, particularly at higher frequency.

(b) *Internal constraints* (Volterra's theory and Touratier's theory). Polynomial expressions are adopted for three displacement components versus coordinates. Volterra's theory was elaborated for isotropic materials. Touratier's theory seems to better describe dispersion phenomenon for composite materials. Maybe there are some limitations at higher frequencies.

c) *Reissner's variational calculus.* Some successful attempts have been made by Touratier in this sense. However, in the framework of material characterization, the volume of calculations is so great that it does not encourage the experimenter to go down this route.

---

9 If longitudinal waves are used to test high damping materials such as a solid propellant or special resins, it is possible that the viscoelastic transition zone is confined to a narrow lower frequency band. Impact tests can be used, as discussed in Chapter 11 of [CHE 10]. The increase of temperature is avoided. Tests at higher frequency, consequently, are not necessary.

To keep this chapter devoted essentially to experimental work, and to a reasonable number of pages, we will present Reisner's variational calculus (and Touratier's work on it) separately in Chapter 15.

11.10. Bibliography

[BIS 52] BISHOP R. E. D., "Longitudinal waves in Beams", *Aeronaut Quarterly*, 3, p.280, 1952.

[CHA 76] CHADWICK P., "The existence of pure surface modes in elastic materials with orthorhombic symmetry", *Journal of Sound and Vibration*, vol.47, n°1, pp.39-52, 1976.

[CHE 10] CHEVALIER, Y and VINH, J.T. (eds), *Mechanics of Viscoelastic Materials and Wave Dispersion*, ISTE, London and John Wiley and Sons, New York, 2010.

[CHR 89] CHREE C., "The equations of an isotropic elastic solid in polar and cylindrical coordinates their solutions and applications", *Trans. Camb. Phil. Soc. Math. Phys.* 14, 250, 1889.

[FRA 69] FRASER W. B., "Stress wave propagation in rectangular bars", *Int. Journ. of Solids and Structures*, Vol.10, pp. 63-73, 1969.

[HER 50] HERMANN G. A., MINDLIN R. D., "One dimensional theory of compressional wave in elastic rods", *Proc. 1st U.S. National Congress Applied Mechanics*, pp. 187-191, 1950.

[HET 68] HETERLENDY P., "An approximate theory governing symmetric motions of elastic rods of rectangular or square section cross-section", *Journal of Applied Mechanics*, Vol. 13, series E, N°2, pp. 333-341, June1968

[KYN 57] KYNCH G. J., GREEN W.A., "Vibrations of beams – I – longitudinal modes", *Quarterly Journal of Mechanics and Applied Mathematics*, vol.10, pp. 63-73, 1957.

[LOV44] LOVE A. E., *A Treatise on the Mathematical of Elasticity,* Dover Publications, New York, Re-edition, 1944.

[MED 66] MEDICK M. A., "One dimensional theory of propagation and vibration in elastic bars of rectangular cross-section", *Journal of Applied Mechanics*, pp. 489-495, September 1966.

[MIN 60] MINDLIN R. D., Mc NIVEN H. D., "Axially symmetric waves in elastic rods", *Journ. of Applied Mechanics*, Vol. 27, pp. 145-151, 1960.

[MIN 66] MINEUR H., *Numerical Calculation Technique*, Dunod, Paris, 1966.

[MOR 50] MORSE R. W., "The velocity of compressional waves in rods of rectangular cross-section", *J. Acoust. Soc. Americ.*, Vol. 22, p. 219, 1950.

[NIG 68] NIGRO N. J., "Wave propagation in anisotropic bars of rectangular cross-section", *J. Acoust. Soc. Americ.*, Vol. 43, n°5, p. 958, 1968.

[POC 76] POCHHAMMER L., "Über die Fortpflanzungsgeschwindigkeiten kleiner Schwingungen in einem übergrenzten isotropen Kreiszylinder", *J. Rein. Angew. Math*. 81, pp. 324-336, 1976.

[RAO 74] RAO K.S, RAO B.R., "Free and forced vibrations of rod according to Bishop's theory", *Journal of the Acoustical Soc. Of America*, vol. 56, n°6, pp. 1792-1800, December 1974.

[RAY 45] RAYLEIGH J. W. S., *The Theory of Sound*, vol. I and vol. II, Dover Publications, New York, 1945.

[ROS 74] ROSENFELD G., KELLER J. B., "Wave propagation in elastic rods of arbitrary cross-section", *J. Acoust. Soc. Americ*., Vol. 55, n°3, pp. 555, 1974.

[TOU 77] TOURATIER M., On the propagation of longitudinal waves on rectangular composite rods. (Rayleigh waves, wave dispersion), Report of final studies to obtain engineer degree, Conservatoire National des Arts et Métiers, Paris, 240 p., In French, 1977.

[TOU 79] TOURATIER M., About the wave propagation in transverse isotropic rod with rectangular cross-section (Utilization of Hellinger-Reissner's variational principle – Theoretical and experimental studies at higher modes), PhD thesis, University of Paris VI, In French, 1979.

[VIK 67] VIKTOROV I. A., *Rayleigh and Lamb Waves,* Plenum Press, New York, 1967.

[VIN 80] VINH T., CHEVALIER Y., GARCEAU P., *Final Reports of Industrial Aerospace Contract*, I.S.C.M., Saint Ouen, France, 1980.

[VOL 55] VOLTERRA E., "A one dimensional theory of wave propagation in elastic rod based in the method of internal constraints", *Ing. Archi. Berlin*, Vol. 23, p. 410, 1955.

[VOL 65] VOLTERRA E., ZACHMANOGLOU E. C., *Dynamics of Vibrations*, Charles Merril books, Columbus Ohio USA, pp. 551-554, 1965.

11.11. Appendix 11A. Eigenvalue equation for rod of finite length

For a rod with finite length, we have to deal with stationary waves and boundary conditions at both ends. To make further handling of equations of motion and related boundary conditions easier, it is convenient to adopt dimensionless equations by introducing rod length L.

The two principal spatial and temporal dimensionless variables are:

$$\eta = \frac{x_3}{L} \text{ and } \tau = \omega t \qquad [11.A.1]$$

x_3 being axial displacement.

There is an unknown function $u_j^{(m,n)}$, where:

$$u_j^{(m,n)}\left(x_3, t\right) = \tilde{u}_j^{(m,n)}\left(\eta, \tau\right) \qquad [11.A.2]$$

As function $u_3^{(0,0)}$ is homogenous to a length, it is possible to write

$$\tilde{u}_3^{(0,0)}\left(\eta, \tau\right) = L\, u_3^{*(0,0)}\left(\eta, \tau\right) \qquad [11.A.3]$$

Equations of motion formulated by Touratier [TOU 77] include three displacement components (see Chapter 7 in [CHE 10]), u_3 being an axial displacement component, and L, b, h the length, width and thickness, respectively:

$$\frac{h^2}{4}\,\omega^2\,\frac{\partial^2\,\tilde{u}_1^{(1,0)}}{\partial\tau^2} = q^2\,\frac{h^2}{4}\,\frac{\chi_{44}^2}{L^2}\,\frac{\partial^2\tilde{u}_1^{(1,0)}}{\partial\eta^2} - \chi_{11}^2\,\tilde{u}_1^{(1,0)} - \chi_{12}^2 u_2^{(0,1)} - \chi_{13}^2\,\frac{\partial u_3^{*(0,0)}}{\partial\eta}$$

$$\frac{b^2}{4}\,\omega^2\,\frac{\partial^2\,\tilde{u}_2^{(0,1)}}{\partial\tau^2} = q^2\,\frac{b^2}{4}\,\frac{\chi_{44}^2}{L^2}\,\frac{\partial^2\tilde{u}_2^{(0,1)}}{\partial\eta^2} - \chi_{11}^2\,\tilde{u}_2^{(0,1)} - \chi_{12}^2 u_1^{(1,0)} - \chi_{13}^2\,\frac{\partial u_3^{*(0,0)}}{\partial\eta}$$

$$L\omega^2\,\frac{\partial^2\,u_3^{*(0,0)}}{\partial\tau^2} = \frac{1}{L}\left\{\chi_{33}^2 - \frac{4\,\chi_{13}^4}{3\left(\chi_{11}^2+\chi_{12}^2\right)}\right\}\frac{\partial^2 u_3^{*(0,0)}}{\partial\eta^2} + \frac{\chi_{13}^2}{3\,L}\left(\frac{\partial\tilde{u}_1^{(1,0)}}{\partial\eta} + \frac{\partial u_2^{(0,1)}}{\partial\eta}\right)$$

[11.A.4]

Coefficient c is defined as $\chi^2 = c_{ij}/\rho$, the square of the velocity of a wave which is either longitudinal [i=j and (i,j) ∈ (1,2,3)] or transverse [i=j and (i,j) ∈ (4,5,6)] and $q^2 = \frac{0.87 + 1.12\nu}{1+\nu}$ (see [CHE 10] section 7.7).

Dividing the above equations by $\frac{h^2}{4}$, $\frac{b^2}{4}$ and L, respectively, and multiplying the three equations, term by term by $\frac{L^2}{\chi_{44}^2}$, the following additional dimensionless parameters are retained:

$$\alpha_1^2 = \frac{\chi_{11}^2}{\chi_{44}^2} = \frac{C_{11}}{C_{44}}$$

$$\alpha_2^2 = \frac{\chi_{12}^2}{\chi_{44}^2} = \frac{C_{12}}{C_{44}}$$

$$\alpha_3^2 = \frac{\chi_{33}^2}{\chi_{44}^2} = \frac{C_{33}}{C_{44}}$$

$$\alpha_4^2 = \frac{\chi_{13}^2}{\chi_{44}^2} = \frac{C_{13}}{C_{44}}$$

$$\gamma^2 = \frac{\omega^2 \, L^2}{\chi_{44}^2} \qquad [11.A.5]$$

and then

$$\beta = \frac{l}{\delta} = \frac{h}{b} \quad , \quad \delta_L = \frac{L}{h} \qquad [11.A.6a]$$

$$\chi_{ij}^2 = \frac{C_{ij}}{\rho} \qquad [11.A.6b]$$

In the third dimensionless equation of propagation [11.A.4], the coefficient of the second derivative with respect to space is written as follows

$$\alpha'^2 = \frac{1}{\chi_{44}^2} \left\{ \chi_{33}^2 - \frac{4 \, \chi_{13}^4}{3 \left(\chi_{11}^2 + \chi_{12}^2 \right)} \right\} = \alpha_3^2 - \frac{4 \, \alpha_4^4}{3 \left(\alpha_1^2 + \alpha_2^2 \right)} \qquad [11.A.7]$$

Finally, the dimensionless propagation equations are:

$$\gamma^2 \, \frac{\partial^2 \tilde{u}_1^{(1,0)}}{\partial \tau^2} = q^2 \, \frac{\partial^2 \tilde{u}_1^{(1,0)}}{\partial \eta^2} - 4\alpha_1^2 \, \delta^2 \, \tilde{u}_1^{(1,0)} - 4\alpha_2^2 \, \delta^2 \, \tilde{u}_2^{(0,1)} - 4\alpha_4^2 \, \delta^2 \, \frac{\partial u_3^{*(0,0)}}{\partial \eta}$$

$$\gamma^2 \frac{\partial^2 \tilde{u}_2^{(0,1)}}{\partial \tau^2} = q^2 \frac{\partial^2 u_2^{(0,1)}}{\partial \eta^2} - 4\alpha_1^2 \delta^2 \tilde{u}_2^{(1,0)} - 4\alpha_2^2 \delta^2 \tilde{u}_1^{(1,0)} - 4\alpha_4^2 \delta^2 \frac{\partial u_3^{*(0,0)}}{\partial \eta}$$

$$\gamma^2 \frac{\partial^2 \tilde{u}_3^{*(0,0)}}{\partial \tau^2} = \alpha'^2 \frac{\partial^2 u_3^{*(0,0)}}{\partial \eta^2} + \frac{\alpha_4^2}{3} \left(\frac{\partial \tilde{u}_1^{(1,0)}}{\partial \eta} + \frac{\partial \tilde{u}_2^{(0,1)}}{\partial \eta} \right) \qquad [11.A.8]$$

where the dimensionless factor g is given by the following equation ([CHE 10] section 7.7):

$$\gamma^2 = \frac{\omega^2 L^2}{\chi_{44}^2}$$

We have to deal with three second order coupled equations of motion. Let us introduce the following notation:

$$d_1 = \left(\frac{1}{\alpha'^2} + \frac{2}{q^2} \right) \gamma^2 + \left(\frac{\alpha_4^4}{3\,\alpha'^2} - \alpha_1^2 \right) \frac{\delta^2}{q^2} \left(1 + \beta^2 \right)$$

$$d_2 = \left(\frac{2}{\alpha'^2} + \frac{1}{q^2} \right) \frac{\gamma^4}{q^2} + \left\{ \frac{\alpha_4^4}{3\,\alpha'^2\, q^2} - \alpha_1^2 \left(\frac{1}{q^2} + \frac{1}{\alpha'^2} \right) \right\} \bullet \left(\frac{1+\beta^2}{q^2} \right) \delta^2 \gamma^2$$
$$+ \left\{ \frac{2\,\alpha_4^4}{3\,\alpha'^2} - \left(\alpha_1^2 + \alpha_2^2 \right) \right\} \left(\alpha_2^2 - \alpha_1^2 \right) \frac{\beta^2 \delta^4}{q^4}$$

$$d_3 = \frac{\gamma^2}{q^4\, \alpha'^2} \left\{ \gamma^4 - \alpha_1^2 \delta^2 \left(1 + \beta^2 \right) \gamma^2 + \left(\alpha_1^4 - \alpha_2^4 \right) \beta^2 \delta^4 \right\}$$

$$s^2 = S' \qquad [11.A.9]$$

By forming the following expression:

$$R' = \left[\frac{1}{3} \left(d_2 - \frac{d_1^2}{3} \right) \right]^3 + \left[\left(\frac{d_1}{3} \right)^3 - \frac{d_1\, d_2}{6} + \frac{d_3}{2} \right]^2 \qquad [11.A.10]$$

the following equation in S' of the third order advantageously replaces [11.A.9]:

$$S'^3 + d_1 S'^2 + d_2 S' + d_3 = 0 \qquad [11.A.11]$$

It is presented in a contracted form and admits real roots. $S^{'}$ is a new variable introduced in [11.A.9] in view of finding a solution to equation [11.A.10].

$$S_1^{'} = 2\left\{-\frac{1}{3}\left(d_2 - \frac{d_1^3}{3}\right)\right\}^{1/2} \cos\frac{1}{3}\,\text{Arc}\cos\left\{\frac{\frac{d_1\,d_2}{3} - d_3 - \frac{d_1^3}{27}}{2\left[-\frac{1}{27}\left(d_2 - \frac{d_1^2}{3}\right)\right]^{1/2}}\right\} - \frac{d_3}{3}$$

$$S_2^{'} = 2\left\{-\frac{1}{3}\left(d_2 - \frac{d_1^3}{3}\right)\right\}^{1/2} \cos\frac{1}{3}\left[\text{Arc}\cos\left\{\frac{\frac{d_1\,d_2}{3} - d_3 - \frac{d_1^3}{27}}{2\left[-\frac{1}{27}\left(d_2 - \frac{d_1^2}{3}\right)\right]^{1/2}}\right\} + 4\pi\right] - \frac{d_3}{3}$$

$$S_3^{'} = 2\left\{-\frac{1}{3}\left(d_2 - \frac{d_1^3}{3}\right)\right\}^{1/2} \cos\frac{1}{3}\left[\text{Arc}\cos\left\{\frac{\frac{d_1\,d_2}{3} - d_3 - \frac{d_1^3}{27}}{2\left[-\frac{1}{27}\left(d_2 - \frac{d_1^2}{3}\right)\right]^{1/2}}\right\} + 2\pi\right] - \frac{d_3}{3}$$

[11.A.12]

We should mention that in [11.A.12] solutions S'_1 , S'_2, S'_3 are similar and differ only in $\left[\text{Arc}\cos[\quad] + \text{angle}\,4\pi \text{ or } 2\pi\right]$; the quantity inside the bracket $0,4\pi,2\pi$ in the second term of [11.A.12] differs.

Solutions for equation [11.A.10] allow the phase velocities of the first three elastodynamic modes to be obtained.

11.12. Appendix 11B. Additional information concerning solutions of Touratier's equations[10]

This chapter is devoted essentially to practical aspects of the material characterization of materials and the incidence of the wave dispersion phenomenon.

10 For details of the presentation of equations of motion by using Hamilton variational principle, see the book written by the same authors [CHE 10] Chapter 7, pp.354- 369. Appendix 11C also presents the principal theoretical results.

For a low frequency range in which wave dispersion is ignored, we have to deal with a well-known second order equation of motion. Eigenvalues are easily obtained when boundary conditions are known.

If we expect to find an eigenvalue solution for a higher frequency range, inevitably, displacement components in the cross-section cannot be neglected. We then abandon the simple field of a unique longitudinal component of displacement for a displacement field with three displacement components. Touratier's theory is presented in detail elsewhere [TOU 77].

In Appendix 11A we have three equations of motion of second order with coupling terms. Uncoupling equations of motion can be obtained by the substitution method. Finally, we obtain a sixth order equation of motion with one longitudinal displacement variable. We have to deal with a sixth order equation, a function of the square of the eigenvalue η^2. A closed form solution is possible using characteristic functions, as we have done for the dynamic bending or torsion of rods. However, the mathematical handling of the equation becomes heavy and time consuming. A matricial solution is better adapted and we adopted numerical matricial handling by computer in our research.

11B.1. *Eigenequation with elementary theory of motion*

Two masses, m_1 and m_2, are attached to each of the free ends, respectively.

The stress vector at z = 0 is:

$$\vec{T}\,(0,t) = -\,\sigma_{zz}\,(0,t)\,\vec{z} \qquad [11.B.1]$$

At z = 0, the boundary condition is:

$$m_1\,\frac{\partial^2 w(0,t)}{\partial t^2} = -ES\,\frac{\partial w\,(0,t)}{\partial z} \qquad [11.B.2]$$

The stress vector at z = L is:

$$\vec{T}\,(L,t) = \sigma_{zz}\,(L,t)\,\vec{z}$$

At z = L, the boundary condition is:

$$m_2 \frac{\partial^2 w(L,t)}{\partial t^2} = ES \frac{\partial w(L,t)}{\partial z} \quad [11.B.3]$$

Bringing $w(z,t)= W(z)e^{j\omega}t$ into the elementary equation of longitudinal vibration of a rod:

$$E \frac{\partial^2 w}{dz^2} - \rho \frac{\partial^2 w}{dt^2} = 0 \quad [11.B.4]$$

$W_n(z)$, n[th] mode of vibration, is the solution of

$$W_n''(z) - \gamma_n'^2 W_n(z) = 0 \quad [11.B.5]$$

where $\gamma_n'^2 = \frac{\rho \omega_n^2 L^2}{E}$ [11.B.6]

Solution of of [11.B.4] can be expressed as a combination of trigonometric functions:

$$W_n(z) = A_n \cos(\frac{\gamma_n' z}{L}) + B_n \sin(\frac{\gamma_n' z}{L}) \quad [11.B.7]$$

ringing boundary conditions [11.B.2] and [11.B.3] into [11.B.7], constant A_n and B_n are solution of the following matrix equation

$$\begin{bmatrix} m_1\gamma_n' & -M \\ m_2\gamma_n' \cos\gamma_n' - M\sin\gamma_n' & m_2\gamma_n' \sin\gamma_n' + M\sin\gamma_n' \end{bmatrix} \begin{bmatrix} A_n \\ B_n \end{bmatrix} = \begin{bmatrix} 0 \\ 0 \end{bmatrix} \quad [11.B.8]$$

where M = ρ S L is the rod mass sample expressed versus density ρ t and the cross-section area S and the rod length L.

In order to provide non trivial solution of equation [11.B.8], the determinant must be equal to 0, and then finally:

$$\operatorname{tg} \gamma'_n = \frac{\left(\bar{m}_1 + \bar{m}_2\right) \gamma'_n}{\bar{m}_1 \, \bar{m}_2 \, \gamma'^2_n - 1} \qquad [11.B.9]$$

Letting:

$$\bar{m}_i = \frac{m_i}{M} \{1,2\}$$